Immunity
Article

Rapid Culling of the CD4$^+$ T Cell Repertoire in the Transition from Effector to Memory

Matthew A. Williams,[1,*] Eugene V. Ravkov,[1] and Michael J. Bevan[2,*]
[1]Department of Pathology, University of Utah, Salt Lake City, UT 84121, USA
[2]Department of Immunology and Howard Hughes Medical Institute, University of Washington, Seattle, WA 98195, USA
*Correspondence: matthew.williams@path.utah.edu (M.A.W.), mbevan@u.washington.edu (M.J.B.)
DOI 10.1016/j.immuni.2008.02.014

SUMMARY

Requirements for CD4$^+$ T cell memory differentiation were analyzed with adoptively transferred SMARTA T cell receptor (TCR) transgenic cells specific for a lymphocytic choriomeningitis virus (LCMV) epitope. LCMV-induced effector and memory differentiation of SMARTA cells mimicked the endogenous CD4$^+$ T cell response. In contrast, infection with a recombinant *Listeria* expressing the LCMV epitope, although resulting initially in massive SMARTA expansion, led to loss of effector function and rapid cell death characterized by high expression of the apoptosis regulator Bim. Defective memory differentiation was seen after stimulation of naive but not memory SMARTA cells, was independent of precursor frequency, and correlated with a lower TCR avidity compared to endogenous responders. In addition, long-lived endogenous CD4$^+$ memory T cells skewed to a higher functional avidity over time. These results support a model in which CD4$^+$ T cell memory differentiation and longevity depend on the strength of the TCR signal during the primary response.

INTRODUCTION

After acute infection, antigen-specific T cells expand as much as 50,000-fold, acquire effector function and mediate clearance of the pathogen. After resolution of the infection, 90%–95% of antigen-specific T cells die, leaving behind a long-lived population of memory T cells that provide protection upon reinfection (Williams and Bevan, 2007; Kaech and Wherry, 2007). Memory T cells possess several properties crucial for their function, including higher frequencies than naive precursors, the ability to rapidly reactivate upon antigen stimulation, wide tissue distribution, and the ability to survive and self-renew for long periods in the absence of cognate antigen.

In recent years, it has become clear that numerous signals during the primary phase of the immune response can impact the differentiation of functional memory. CD4$^+$ T cells are thought to deliver signals important for the survival and protective function of ensuing CD8$^+$ memory T cells, even though the primary CD8$^+$ T cell response to a pathogen is often unaffected by their absence (Janssen et al., 2003; Shedlock and Shen, 2003; Sun and Bevan, 2003). Interleukin-2 (IL-2) signals have also been shown to play an important role in the differentiation of memory cells capable of secondary expansion (Williams et al., 2006; Bachmann et al., 2007). Expression of IL-7Rα on T cells at the peak of the effector response to acute infection correlates with the ability to survive the contraction phase and progress to memory (Kaech et al., 2003), although IL-7 signals themselves do not appear to be sufficient for this process (Hand et al., 2007; Klonowski et al., 2006; Sun et al., 2006). These findings have illustrated the need to accurately define the signals during the primary response that promote the differentiation of memory cells with their distinctive properties.

The role of T cell receptor (TCR) signals in the development of memory T cells is not fully understood. In one proposed scenario, repeated encounters with antigen drive the continued expansion and differentiation of T cell populations, with higher degrees of TCR stimulation driving the differentiation to memory (Gett et al., 2003; Lanzavecchia and Sallusto, 2002). However, another model proposes that once the initial encounter with antigen has reached a certain activation threshold, responding T cells expand and differentiate independently of further TCR signals (Prlic et al., 2007). In support of this, CD8$^+$ T cells stimulated with antigen for a short period in vivo or in vitro can undergo expansion, gain effector function, and differentiate to memory (Kaech and Ahmed, 2001; Mercado et al., 2000; van Stipdonk et al., 2003). In vivo antigenic recognition of as little as 6–12 hr, in the context of an inflammatory response, is sufficient to drive effector and memory CD8$^+$ T cell development (Prlic et al., 2006). Inflammatory signals themselves during viral or bacterial infections also preferentially promote the development of end-stage effectors over memory cells (Joshi et al., 2007; Pearce and Shen, 2007).

Evidence indicates that the requirements for effector and memory differentiation differ for CD4$^+$ and CD8$^+$ T cells. A shortened period of stimulation in vivo does not impact the development of the CD8$^+$ T cell effector response but results in a greatly decreased CD4$^+$ T cell response (Obst et al., 2005; Williams and Bevan, 2004), implying a role for continued antigen stimulation in the development of CD4$^+$ T cell responses. Furthermore, in some instances CD4$^+$ memory T cells have shown a gradual decline over time after acute infection in mice, in contrast to the stability of CD8$^+$ memory T cell populations (Homann et al., 2001). This seems to conflict with observations of CD4$^+$ memory T cells in humans, which persist for up to 75 years with a half-life similar to that seen for CD8$^+$ memory T cells (Hammarlund et al., 2003). Understanding the differentiation and maintenance of

$CD4^+$ memory T cells after infection remains an important focus of study, particularly because it relates to the development of vaccine strategies for the targeted stimulation of $CD4^+$ T cell responses.

We employed a model of adoptive transfer of TCR transgenic T cells to study $CD4^+$ T cell memory differentiation in vivo. SMARTA mice express a TCR transgene with specificity for the immunodominant I-A^b-restricted $GP_{61–80}$ epitope of lymphocytic choriomeningitis virus (LCMV). Small numbers (10^3–10^4) of naive $CD4^+$ SMARTA T cells (Thy1.1^+) transferred into C57BL/6 (B6) hosts expanded dramatically after LCMV infection. They also differentiated into cytokine-producing effector cells and long-lived memory cells similarly to endogenous $CD4^+$ T cell responders specific for the same epitope. After infection with a recombinant *Listeria monocytogenes* secreting $GP_{61–80}$ (Lm-gp61), naive SMARTA cells also expanded dramatically (10,000- to 20,000-fold). After resolution of the Lm-gp61 infection, however, SMARTA cells rapidly lost cytokine-producing function and failed to differentiate into memory, despite the development of readily detectable memory populations by endogenous responders to the same epitope in the same animal. As early as day 5 p.i., SMARTA cells were doomed to die and could not be rescued through further stimulation. Only naive SMARTA cells failed to form memory. Memory SMARTA cells initially generated during LCMV infection and then rechallenged with Lm-gp61 readily expanded, differentiated, and formed secondary memory populations. Microarray analysis revealed that the failure to differentiate into memory coincided with increased Bim and decreased Bcl-2 expression at the peak of the response. To assess the role of antigen availability in driving $CD4^+$ T cell differentiation in these two model systems, we measured the functional avidity of endogenous and SMARTA CD4 responders after infection, as defined by the dose of antigen required to elicit a functional response (i.e., IFNγ production). Failure of the SMARTA cells to differentiate into memory correlated with decreased functional avidity as compared to the endogenous Lm-gp61 responders in the same host, suggesting that the limited antigen available during Lm-gp61 infection was insufficient to promote SMARTA memory differentiation. In addition, long-lived $CD4^+$ memory T cell populations (>6 months) were characterized by the emergence of cells with higher functional avidity. These data support a model in which the differentiation of effector and memory $CD4^+$ T cells, as well as the longevity of the ensuing $CD4^+$ memory T cell population, is driven by the strength of antigen stimulation during the primary response.

RESULTS

SMARTA Cells Mimic the Endogenous $CD4^+$ T Cell Response to LCMV

In order to track in vivo $CD4^+$ T cell responses to acute infection, we employed an adoptive-transfer system utilizing SMARTA $CD4^+$ TCR transgenic T cells. We transferred 1×10^4 congenically marked (Thy1.1^+) $CD44^{lo}$ SMARTA cells specific for the I-A^b-restricted $GP_{61–80}$ epitope of LCMV into B6 hosts 1 day prior to LCMV infection. SMARTA cells expanded dramatically during the first week of infection in the spleen (Figure 1A), lymph nodes, and peripheral tissues such as the lung and liver (data not shown). By day 30 p.i., the majority of the SMARTA cells died, leaving behind a long-lived memory population. The memory maintenance phase was characterized by a gradual decline in SMARTA numbers, although substantial numbers of SMARTA cells were readily detectable in the spleen up to 385 days p.i. The rate of decline in memory cell numbers also decreased over time (Figure 1A). The overall kinetics of the SMARTA response to LCMV infection largely mirrored the polyclonal endogenous $CD4^+$ T cell response to the same $GP_{61–80}$ epitope (data not shown).

In addition to displaying similar kinetics, the functional development of the SMARTA cells was similar to that of the endogenous $CD4^+$ T cell responders in the same animal. At both the peak of the effector response (day 8 p.i.) and at memory time points, the bulk of the SMARTA cells maintained the ability to produce Interferon-γ (IFNγ), IL-2, and tumor necrosis factor-α (TNFα), with a cytokine production profile similar to that of the endogenous $CD4^+$ T cell responders (Figure 1B). Combined with the kinetics of the SMARTA response, these results led us to conclude that SMARTA cells could be used as an effective surrogate for endogenous $CD4^+$ T cell responses during LCMV infection (Whitmire et al., 2006).

SMARTA Cells Expand and Differentiate after Lm-gp61 Infection but Fail to Form Memory

In order to study SMARTA differentiation in another model system, we infected host mice with recombinant *Listeria monocytogenes* expressing the I-A^b-restricted $GP_{61–80}$ epitope of LCMV under the control of the LLO promoter (Lm-gp61). By day 8 p.i., SMARTA cells had expanded dramatically, although they were present at lower frequencies and total numbers in the spleen than SMARTA cells 8 days after LCMV infection. By day 60, however, SMARTA cells had completely disappeared from the spleens of Lm-gp61-infected animals (Figures 2A and 2D). In contrast, after either infection, endogenous $CD4^+$ T cell responders in the same animal specific for the same epitope were readily detectable at the peak of the response (day 8 p.i.) and at memory time points (day 60) (Figures 2B and 2D). Similar results were found in the liver (data not shown). A closer look at the day 8 response to Lm-gp61 revealed that although the SMARTA cells expanded several thousand fold during the first week of infection, they failed to differentiate properly in comparison to the endogenous responders, as measured by their ability to produce cytokines. Whereas the great majority of IFNγ-producing endogenous $CD4^+$ T cell responders also produced TNFα and IL-2, only a small proportion of SMARTA cells at this time point retained this ability (Figure 2C). Furthermore, production of all three cytokines by SMARTA cells in response to peptide stimulation was much lower, as measured by mean fluorescence intensity of intracellular staining.

We analyzed the kinetics and cytokine profile of the SMARTA response in greater detail during the first 2 weeks after Lm-gp61 infection (Figure 3A). SMARTA cells were readily detectable at 5 days p.i. Furthermore, at this early stage, their ability to produce both IFNγ and TNFα mirrored that of the endogenous responders. Although they continued to expand until day 7 p.i., most of the SMARTA cells lost the ability to produce TNFα between day 5 and day 7, as compared to the endogenous $CD4^+$ T cell responders that retained the ability to secrete high amounts of both cytokines. We observed a similar decline in

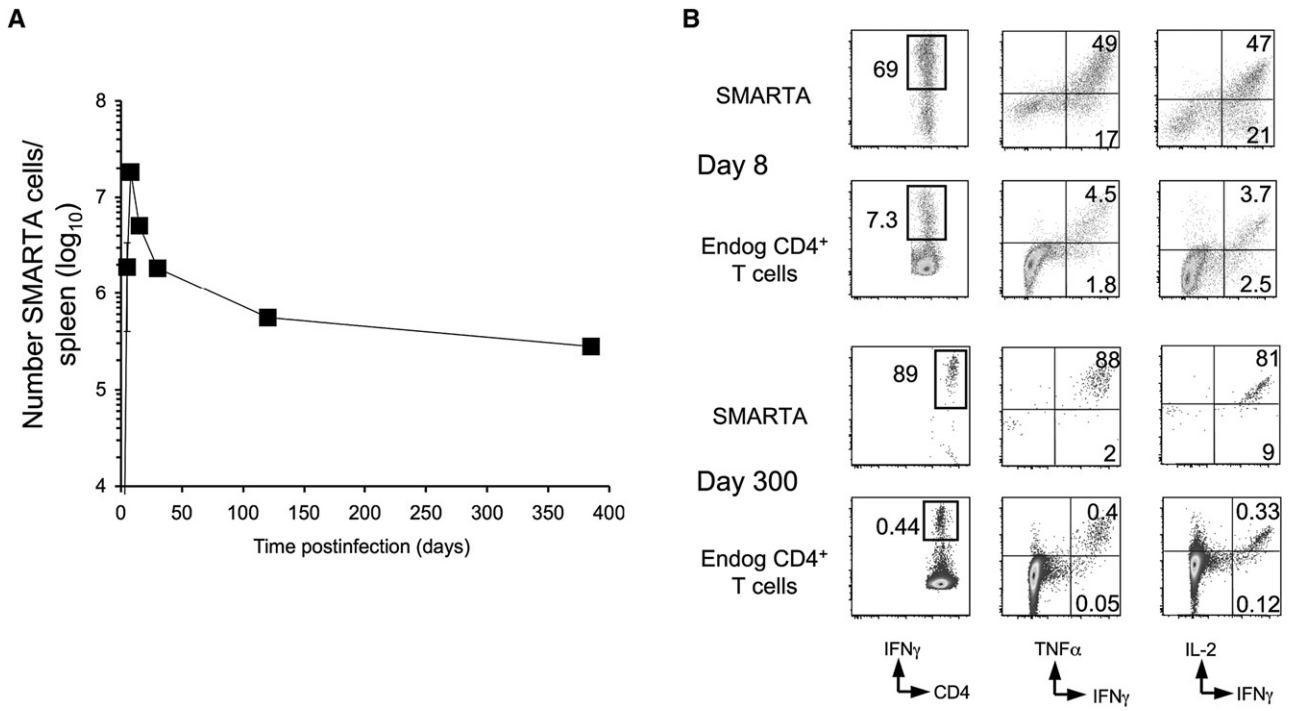

Figure 1. Adoptively Transferred SMARTA Cells Mimic the Endogenous CD4+ T Cell Response to LCMV

(A) Thy1.1+CD44lo SMARTA cells (1×10^4) were transferred into B6 hosts (Thy1.2+). Mice were infected with LCMV 1 day later, and the subsequent expansion, contraction, and memory maintenance of SMARTA cells in the spleen were calculated on the basis of expression of Thy1.1. Error bars display the standard error of the mean (SEM) (n = 3–4 per time point), and results are representative of four different experiments.

(B) Splenocytes harvested at day 8 or day 300 p.i. were restimulated with $GP_{61–80}$ peptide for 4 hr in the presence of Brefeldin A. Cells were then stained for intracellular expression of IFNγ, TNFα, and IL-2. We gated on CD4+ Thy1.1+ SMARTA responders and CD4+Thy1.1− endogenous responders from the same animal and assessed their ability to make each cytokine at each time point. Flow plots are representative of effector and memory time points over the course of four time-course experiments.

the ability of SMARTA cells to produce IL-2 between days 5 and 7 (data not shown). Whereas the number of endogenous responders declined slowly through the contraction phase until day 15 p.i., SMARTA numbers dropped precipitously. At day 12 they represented only 0.1% of the CD4 population, and by day 15 they were undetectable (Figure 3A). Furthermore, rechallenge with LCMV at day 5 p.i. with Lm-gp61 failed to rescue the SMARTA cells, for under these conditions SMARTA cells were still undetectable by day 15 p.i. (Figure S1 available online). These data indicated that not only were SMARTA cells progressively losing functional capacity by days 5–7 p.i., but they were also irreversibly committed to undergoing programmed cell death.

We asked whether memory SMARTA cells generated by LCMV infection could form secondary memory after rechallenge with Lm-gp61. Infection with LCMV gave rise to a readily detectable SMARTA memory population 180 days later, with frequencies ranging from 0.2% to 1.0% of CD4+ T cells in the spleen, lymph nodes, and liver (data not shown). After rechallenge with Lm-gp61 at this time point, SMARTA memory cells expanded dramatically, differentiated normally as measured by IFNγ and TNFα production, and differentiated to readily detectable secondary memory by day 42 after rechallenge (Figure 3B). As a control for this experiment, mice receiving naive SMARTA cells and given a primary challenge with Lm-gp61 failed to develop detectable SMARTA memory cells at day 42 p.i. (data not shown). Therefore, unlike naive SMARTA cells, memory SMARTA cells do have the ability to differentiate to secondary memory after Lm-gp61 infection.

Failed SMARTA Memory Differentiation Is Independent of Precursor Frequency

We next considered the possibility that the inability of SMARTA to differentiate into memory after Lm-gp61 infection could depend on the precursor frequency of responding cells. Clonal competition has been shown to play an important role in the selection, differentiation, and survival of CD4+ T cell responders in vivo (Foulds and Shen, 2006). We hypothesized that after Lm-gp61 infection, competition for limited access to antigen or to differentiation and growth factors due to abnormally high precursor frequencies might prevent normal memory differentiation of the SMARTA cells. By assuming a "take" of ~10% of adoptively transferred cells, as confirmed with high-frequency transfers (data not shown), we estimated that our previous transfers of 1×10^4 SMARTA cells resulted in a precursor frequency of ~1×10^3, or roughly 5–20-fold higher than the estimated endogenous precursor frequency for this epitope (Whitmire et al., 2006).

To test the possibility that clonal competition prevented SMARTA memory differentiation, we transferred 1×10^3, 1×10^4, or 1×10^5 SMARTA cells into naive B6 mice that were

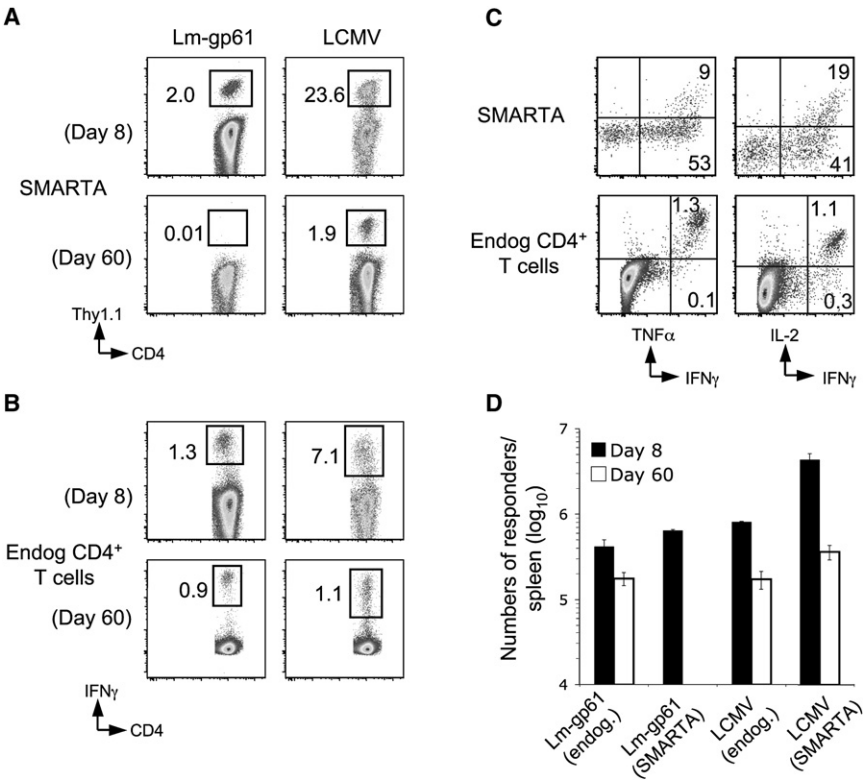

Figure 2. SMARTA Cells Expand but Fail to Gain Full Effector Function and Form Memory after Lm-gp61 Infection

(A) Thy1.1$^+$CD44^{lo} SMARTA cells (1×10^4) were transferred into B6 hosts (Thy1.2$^+$). Mice were infected with Lm-gp61 or LCMV 1 day later, and the expansion, contraction, and memory maintenance of SMARTA cells in the spleen were assessed. Representative flow plots display the frequency of Thy1.1$^+$CD4$^+$ SMARTA cells in the spleen at day 8 and day 60 p.i. for each infection.

(B) Representative flow plots display the frequency of IFNγ-producing endogenous CD4$^+$ responders (CD4$^+$Thy1.1$^-$) in the spleen after peptide restimulation in the presence of Brefeldin A.

(C) Representative flow plots compare the ability of SMARTA cells (CD4$^+$Thy1.1$^+$) and endogenous CD4$^+$ responders (CD4$^+$Thy1.1$^-$) in the spleen to make IFNγ, TNFα, and IL-2 after peptide restimulation at day 8 p.i. Flow plots are representative of six separate experiments.

(D) The number of SMARTA (Thy1.1$^+$) and endogenous (IFNγ-producing) responders in the spleen are shown for day 8 and day 60. Error bars represent the SEM (n = 3 per group).

infected with Lm-gp61 1 day later. At day 7 p.i., SMARTA cells were readily detectable in the spleens of all groups, with the highest frequencies and largest numbers harvested from the group that received 1×10^4 SMARTA cells (Figures 4A and 4B). However, the greatest expansion was observed in the group that received 1×10^3 SMARTA cells. Assuming a 10% "take" and estimating an actual precursor frequency of ~100 SMARTA cells in this group (which is similar to that of endogenous precursor frequencies), we calculated a 12,000- to 16,000-fold expansion by SMARTA cells during the first 7 days after Lm-gp61 infection (Figure 4C). Remarkably, however, such massive expansion was not accompanied by enhanced differentiation, as measured by their ability to make IFNγ, TNFα, and IL-2 (data not shown), nor did it confer the properties necessary for memory generation,

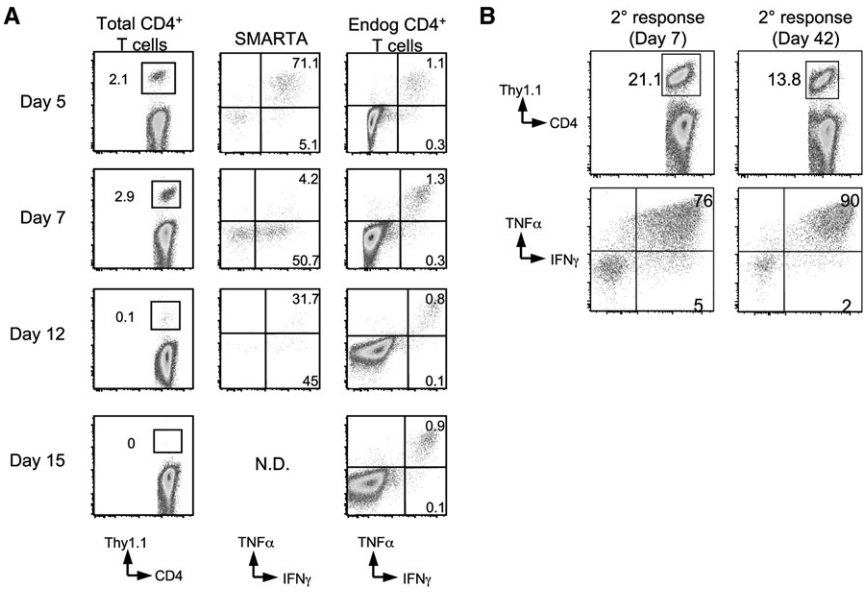

Figure 3. After Lm-gp61 Infection, Naive SMARTA Cells Lose Function and Disappear whereas Memory SMARTA Differentiate Normally

(A) Thy1.1$^+$CD44^{lo} SMARTA cells (1×10^4) were transferred into B6 hosts (Thy1.2$^+$). Mice were infected with Lm-gp61 1 day later, and SMARTA cells were subsequently tracked in the spleen at several time points p.i. on the basis of Thy1.1 expression (left column). Cytokine production by SMARTA (middle column) and endogenous (right column) CD4$^+$ T cell responders from the same animal was assessed at the indicated points. Flow plots are representative of three mice per time point in this experiment, and similar results were found in three separate experiments.

(B) Thy1.1$^+$CD44^{lo} SMARTA cells (1×10^4) were transferred into B6 hosts (Thy1.2$^+$). Mice were infected with LCMV 1 day later and then rechallenged with Lm-gp61 180 days after the primary infection. Representative flow plots display the frequency of SMARTA cells in the spleen at 7 and 42 days after rechallenge (top row). The bottom row displays the ability of SMARTA cells at each time point to produce IFNγ and TNFα in response to ex vivo peptide restimulation. Plots are representative of 3–4 mice per group.

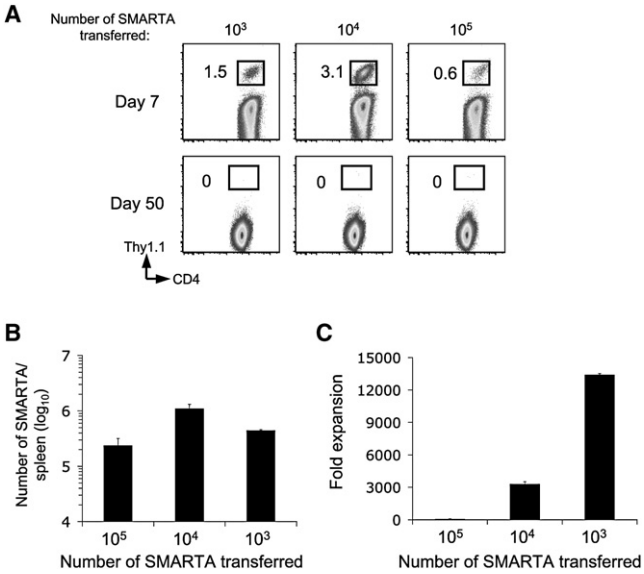

Figure 4. SMARTA Cells Fail to Differentiate into Memory after Lm-gp61 Infection Regardless of Naive-Precursor Frequency

(A) Thy1.1$^+$CD44^{lo} SMARTA cells (1×10^3, 1×10^4, or 1×10^5) were transferred into B6 hosts (Thy1.2$^+$) that were infected with Lm-gp61 1 day later. Representative flow plots display the frequency of Thy1.1$^+$ SMARTA cells among total CD4$^+$ T cells at days 7 and 50 p.i. for each cell dose.

(B) Bar graph displays the number of SMARTA cells harvested at day 7 p.i. after transfer of the indicated number of naive SMARTA cells.

(C) Bar graph displays the n-fold expansion of SMARTA cells at each cell dose during the first week p.i. Starting numbers were calculated on the basis of a 10% "take" of transferred cells. Error bars represent the SEM (n = 3 per group).

as evidenced by our observation that SMARTA cells were undetectable in all groups by day 50 p.i. regardless of precursor frequency (Figure 4A). Therefore, we concluded that the signals required for CD4$^+$ T cell memory differentiation can be disassociated from those required for robust clonal expansion during the primary phase of the response. Furthermore, clonal competition could not be invoked to explain the inability of SMARTA cells to form memory after Lm-gp61 infection.

SMARTA Gene-Expression Profile

In order to explore the mechanism leading to the death of SMARTA responders after Lm-gp61 infection, we analyzed the gene-expression profiles of SMARTA cells 7 days after infection with either LCMV or Lm-gp61 via gene-expression microarrays (Tables 1 and 2). This analysis demonstrated stark differences in the gene-expression profile of SMARTA cells responding to each type of infection. SMARTA cells after Lm-gp61 infection demonstrated increased expression of 65 genes of known function (as defined by an average $\geq$ 3-fold increase in expression in two separate experiments). Of these, 45 encoded gene products with known suppressive or regulatory activities as transcriptional repressors (e.g., TSC-22, Tob2), inhibitors of cell cycle or cellular activation (e.g., Rap2A, Unc5cl, PP2A, Ptger4), or proapoptotic factors (e.g., Bim, Nor-1, FoxO3a, FasL). In contrast, after LCMV infection, over 300 genes demonstrated increased expression, including genes that encode antiapoptotic factors (e.g., Bcl-2, Hsp110, SODD), growth and activation factors (e.g., β-catenin, TCF-1, CD27, CD122), trafficking receptors (e.g., CXCR5, CD43), and gene products involved in metabolic pathways, cell cycling, chromatin remodeling, transcription and cellular activation, and regulation of TCR signals and cellular growth. These data indicate that SMARTA cells at day 7 after Lm-gp61 infection are undergoing apoptosis and are refractory to activation signals. Of particular interest is the discoordinated expression of the genes encoding Bim and Bcl-2, two molecules that have been shown to have opposing effects on T cell survival during various phases of the immune response (Marrack and Kappler, 2004). The microarray results for Bcl-2, β-catenin, TCF-1, Nor-1, and Bim have been further confirmed by real-time PCR (Figure S2). Intracellular staining also revealed decreased Bcl-2 protein expression after Lm-gp61 infection (Figure S2).

Together, these data strongly suggest that stimulation of the SMARTA cells during Lm-gp61 infection induces rapid expansion but defective differentiation and eventual programmed cell death. Given the rapid disappearance of the SMARTA cells, one concern was that they are rejected during *Listeria* infection, whether as a result of the expression of the Thy1.1 congenic marker or minor histocompatibility differences not eliminated during backcrossing. Several lines of evidence indicate that this is not the case. First, the loss of function as reflected by cytokine production is indicative of failed differentiation, not rejection. Second, the gene-expression profile is also indicative of failed differentiation and programmed cell death, with increased expression of key apoptotic factors. Third, memory SMARTA challenged with Lm-gp61 readily form secondary memory, indicating that the failure of naive SMARTA to form primary memory after stimulation is probably due to differences in activation threshold, not rejection. To definitively address the issue of rejection, we transferred day 8 SMARTA from either Lm-gp61- or LCMV-infected hosts into secondary hosts that were also day 8 p.i. with either Lm-gp61 or LCMV and that had also received an initial SMARTA transfer prior to infection (to ensure that the mice were "primed"). In order to distinguish the secondary SMARTA transfer from the initial SMARTA transfer in these hosts, we labeled the transferred SMARTA cells with CFSE. Seven days later (15 days p.i.), the survival of SMARTA cells in the spleen was assessed. Although some CFSE dilution was observed, primary and secondary SMARTA transfers were distinguishable. As expected, SMARTA cells generated in a Lm-gp61-infected host and injected into a Lm-gp61-infected host largely disappeared, whereas SMARTA cells generated in a LCMV-infected host and transferred into a LCMV-infected host were readily detectable. Conversely, SMARTA cells generated in a Lm-gp61-infected host and injected into a LCMV-infected host disappeared within 7 days, whereas SMARTA cells generated in a LCMV-infected host and transferred into a Lm-gp61-infected host demonstrated no impairment in survival (Figure S3). We were therefore unable to detect any mechanism for rejecting SMARTA cells in Lm-gp61-infected animals and definitively ruled out this possible explanation for their disappearance.

Failed SMARTA Memory Differentiation Correlates with Low Functional Avidity

Previous studies have indicated that CD4$^+$ T cells undergo avidity maturation throughout the primary response to pathogen as

Table 1. Upregulated Gene Expression in SMARTA Responders 7 Days after Infection with Lm-gp61

Gene Product	n-Fold Increase	Function	Reference
Bim	12	apoptosis	(Marrack and Kappler, 2004)
Nor-1	8	TCR-induced apoptosis	(Cheng et al., 1997)
FoxO3a	5	tolerance, apoptosis	(Lin et al., 2004; Stahl et al., 2002)
FasL	7	apoptosis, AICD	(Green et al., 2003)
Unc5cl	4	apoptosis (death domain), inhibits NF-kB	(Zhang et al., 2004)
Bach-2	9	transcriptional repressor, apoptosis	(Muto et al., 2002)
TSC-22	5	transcriptional repressor of activation, proliferation	(Kester et al., 1999)
Ssbp2	4	transcriptional repressor of growth and differentiation	(Liang et al., 2005)
Zfhx1a	3	transcriptional repressor, cell cycle arrest	(Chen et al., 2006)
Tis7	3	transcriptional repressor	(Vietor and Huber, 2007)
Tob2	3	transcriptional repressor of T cell activation	(Jia and Meng, 2007)
FoxN3	3	transcriptional repressor of tumorigenic genes	(Scott and Plon, 2005)
Rap2A	7	prevents Akt activation	(Christian et al., 2003)
PP2A	5	suppresses CTLA4-mediated Akt signals	(Parry et al., 2005)
Smad2	4	TGFβ signaling	(Mamura et al., 2000)
March7	3	suppresses T cell activation, proliferation (Ub. ligase)	(Metcalfe et al., 2005)
SLAP	3	TCR degradation	(Myers et al., 2005)
Pdcd4	3	programmed cell death, AP-1 inhibitor	(Bitomsky et al., 2004)
Ptger4	3	suppresses CD4 T cell activation	(Kabashima et al., 2002)
Cyclin D2	4	cell cycle	
PI3K	3	TCR-induced T cell activation	

Genes whose upregulated expression is induced by Lm-gp61. Approximately 70% of upregulated mRNA with gene products of known function encode genes with described or predicted involvement in suppression of cell proliferation, activation, differentiation, or promotion of apoptosis (45/65).

Table 2. Upregulated Gene Expression in SMARTA Responders 7 Days after Infection with LCMV

Gene Product	n-Fold Increase	Function	Reference
Bcl-2	8	antiapoptotic	(Marrack and Kappler, 2004)
SODD	4	silencing of death domains, anti-apoptotic	(Jiang et al., 1999)
Hsp110	11	stress response, survival	(Yamagishi et al., 2006)
β-catenin	9	T cell survival, proliferation	(Qiang and Rudikoff, 2004)
TCF-1	8	T cell survival, proliferation	(Qiang and Rudikoff, 2004)
CD27	5	T cell survival, differentiation	(Hendriks et al., 2003)
CD122	3	T cell growth, survival	(Waldmann, 2006)
CD43	9	T cell expansion, migration	(Onami et al., 2002)
CXCR5	9	T cell trafficking to germinal center	(Breitfeld et al., 2000; Schaerli et al., 2000)

Genes whose upregulated expression is induced by LCMV. More than 300 genes of known function demonstrated upregulated expression (data not shown) and can generally be segregated into the following categories: stress response/DNA repair; metabolic pathways; cell-cycle signaling pathways of cellular activation, proliferation, and survival; chromatin structure; trafficking receptors (e.g., CXCR5); growth/survival factor receptors (e.g., CD122); negative regulators of TCR-mediated signaling; and transcription factors associated with cellular activation.

well as during subsequent rechallenges (Savage et al., 1999; Whitmire et al., 2006). These results support the idea that $CD4^+$ T cell effector differentiation and the selection of responding repertoires is driven at least in part by the strength of antigenic stimulation. Furthermore, the observation that memory SMARTA challenged with Lm-gp61 readily differentiated into secondary memory suggested the possibility that their ability to differentiate could be due to the lower activation threshold of memory cells. Therefore, we hypothesized that the density of antigen on the APC could also impact the selection of $CD4^+$ T cell responders for differentiation into memory. In this scenario, a certain degree of TCR stimulation might be required for clonal expansion, but further stimulation would be required for memory differentiation. In our model system, high antigen density provided by LCMV infection might promote the expansion and differentiation of $CD4^+$ T cell responders over a wider range of functional avidities, whereas lower antigen density provided by Lm-gp61 infection might allow memory differentiation of only high functional avidity responders. SMARTA cells, if they were of low avidity, would be able to initially expand and differentiate after Lm-gp61 infection but would lack sufficient TCR signals to progress to memory.

We tested this hypothesis by measuring the functional avidities of SMARTA and endogenous $CD4^+$ T cell responders at the peak of the primary response to either LCMV or Lm-gp61. The functional avidity of the responding populations was measured by assessing their ability to produce IFNγ ex vivo in

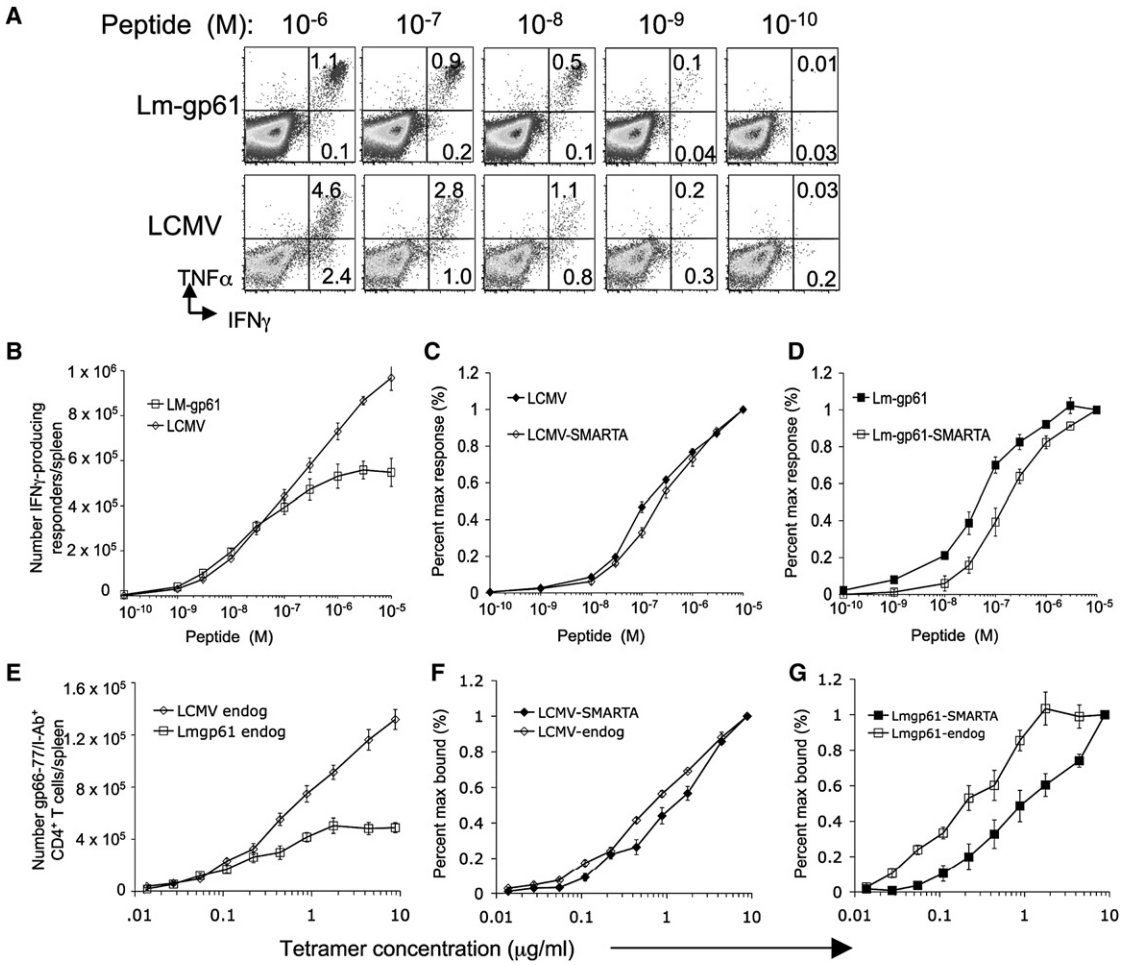

Figure 5. SMARTA Responders Demonstrate Lower Functional Avidity, as Compared to Endogenous CD4$^+$ T Cell Responders to Lm-gp61 in the Same Host

(A) B6 mice were infected with either LCMV or Lm-gp61. Eight days later, splenocytes were restimulated over a range of $GP_{61–80}$ peptide concentrations and stained for expression of IFNγ and TNFα. Representative flow plots are gated on CD4$^+$ T cells and show the frequency of cytokine producers after restimulation at the indicate peptide concentrations.

(B) The graph displays the number of endogenous CD4$^+$ T cells in the spleen capable of producing IFNγ in response to decreasing concentrations of peptide.

(C) Thy1.1$^+$CD44^{lo} SMARTA cells (1×10^4) were transferred into B6 hosts (Thy1.2$^+$), and mice were infected with LCMV 1 day later. The graph displays the percent maximal endogenous or SMARTA CD4$^+$ T cell response induced by ex vivo peptide restimulation, as measured by the frequency of IFNγ-producing responders at each peptide concentration divided by the frequency of IFNγ-producing responders at the highest peptide concentration (1×10^{-5} M).

(D) Thy1.1$^+$CD44^{lo} SMARTA cells (1×10^4) were transferred into B6 hosts (Thy1.2$^+$), and mice were infected with Lm-gp61 1 day later. The graph displays the percent maximal endogenous or SMARTA CD4$^+$ T cell response induced by ex vivo peptide restimulation, as measured by the frequency of IFNγ-producing responders at each peptide concentration divided by the frequency of IFNγ-producing responders at the highest peptide concentration (1×10^{-5} M). The error bars represent the SEM (n = 3 per group). Results are representative of four separate experiments.

(E) Thy1.1$^+$CD44^{lo} SMARTA cells (1×10^3) were transferred into B6 hosts (Thy1.2$^+$), and mice were infected with LCMV or Lm-gp61 1 day later. Decreasing concentrations of $gp_{66–77}$:I-A_b class II tetramer was used to stain SMARTA and endogenous responders at day 8 p.i. The graph displays the number of tetramer-positive endogenous cells detected at each concentration, normalized to staining with the control tetramer hCLIP/I-A^b.

(F and G) The graph displays the percentage of tetramer-positive cells as compared to the number of tetramer-positive cells at the highest tetramer concentration after LCMV or Lm-gp61 infection. Error bars represent the SEM (n = 4 per group).

response to decreasing concentrations of their cognate peptide, $GP_{61–80}$. The maximal I-A^b-$GP_{61–80}$-restricted response was detected with 10^{-5} M peptide. With decreasing peptide concentrations, the number of endogenous CD4$^+$ T cell responders after LCMV infection began to decrease immediately, showing a half-maximal response between 1×10^{-7} M and 3×10^{-7} M peptide. In contrast, virtually all endogenous responders generated after Lm-gp61 infection were able to respond at peptide concentrations as low as 3×10^{-7} M, and they displayed a half-maximal response at one-fifth to one-tenth the concentration of peptide (Figures 5A and 5B). Whereas LCMV induced effectors that required high concentrations of peptide for their functional activity (1×10^{-7} M to 1×10^{-5} M), this population was absent in the Lm-gp61-infected animals (Figure 5B). These results indicated that LCMV infection was able to recruit both intermediate- and high-functional-avidity responders, whereas

Lm-gp61 infection resulted in the effector differentiation of only high-avidity cells, supporting the idea that higher amounts of antigen are available during LCMV infection.

We then asked where SMARTA responders fell in the functional-avidity spectrum. SMARTA effector cells generated after LCMV infection demonstrated a similar range of functional avidities as compared to the endogenous responders in the same host (Figure 5C). SMARTA effector cells generated after Lm-gp61 infection, in contrast, displayed decreased functional avidity as compared to the endogenous Lm-gp61 responders to the same epitope in the same host (half-maximal responses induced by peptide concentrations of $\sim$2 x10^{-7} M for SMARTA responders and $\sim$5 × 10^{-8} M for endogenous CD4 responders) (Figure 5D).

Failed SMARTA Differentiation Corresponds to Low TCR Avidity

Because it is possible that differences in functional avidity may not reflect differences in actual TCR avidity, we also assessed the ability of SMARTA and endogenous responders to bind class II tetramers for this epitope (gp_{66-77}:I-A^b). We found that tetramer staining of both LCMV and Lm-gp61 endogenous $CD4^+$ T cell responders was similar in frequency to the number of responders detected via intracellular cytokine staining (Figure S4). We then tested the ability of both SMARTA and endogenous responders to bind decreasing concentrations of tetramer in an equilibrium binding assay. All staining was normalized to the negative control tetramer, hCLIP:I-A^b. As with the functional-avidity assays, we found that after LCMV infection, the number of tetramer-binding cells began to decrease as soon as the tetramer was diluted below 8 μg/ml. In contrast, the number of Lm-gp61 responders binding tetramer remained stable at one-fourth the concentration and then began to decline as tetramer was diluted further (Figure 5E). We compared the ability of SMARTA and endogenous responders to bind tetramer by calculating the number of tetramer-positive cells at each concentration as a percentage of tetramer-positive cells at the highest concentration. These results again corresponded to those obtained with the functional-avidity assay. The ability of SMARTA cells to bind tetramer in LCMV-infected hosts mirrored that of the endogenous responders (Figure 5F), whereas the ability of SMARTA cells to bind tetramer in Lm-gp61-infected hosts was lower than that of the endogenous responders (Figure 5G). We plotted our results with Scatchard analysis and calculated apparent K_D as previously described (Savage et al., 1999). This revealed that whereas the apparent K_D of SMARTA cells after LCMV infections was similar to endogenous responders in the same host (17.1 nM versus 16.6 nM), the K_D of endogenous responders to Lm-gp61 was significantly lower (3.2 nM) than either SMARTA responders in the same host (18.3 nM, $p = 0.01$) or endogenous responders to LCMV (16.6 nM, $p = 0.02$) (Figure S5). Our results indicate that the inability of SMARTA cells to form memory corresponds to a decreased ability to compete for TCR signals. These findings support the idea that decreased availability of antigen during Lm-gp61 infection is sufficient to drive expansion and partial effector differentiation of SMARTA cells but is not sufficient for their differentiation into memory.

One possible explanation for these results is that responders to each pathogen are recognizing slightly different determinants of the gp_{61-80} epitope. Because the tetramer only incorporates the gp_{66-77} 12-mer, we find this explanation unlikely. The frequency of tetramer-binding cells in each infection corresponded to the number of IFNγ-producing cells after gp_{61-80} peptide restimulation. Furthermore, the avidity, as measured with the tetramer, corresponded to the functional avidity, as measured with the 20-mer gp_{61-80} (Figure 5). These results indicate that the repertoire of responding cells in each type of infection is probably responding to the same epitope. As a preliminary analysis or TCR repertoires, we analyzed Vβ usage by tetramer-positive cells (Figure S6). We found two staining patterns: subsets that stained an equal number of LCMV and LM-gp61 responders (Vβ2,3,5,6,13) and subsets that stained more LCMV responders than Lm-gp61 responders (Vβ4,7,8.1/8.2,8.3,14). We did not observe any unique Vβ-subset usage by Lm-gp61 responders. These findings are consistent with the idea the Lm-gp61-responding repertoire is a subset of the LCMV-responding repertoire.

Functional-Avidity Maturation of Long-Lived $CD4^+$ T Cell Memory

By analyzing the functional avidities of the endogenous $CD4^+$ T cell memory populations after either LCMV or Lm-gp61 infection, we further explored the role of signal strength during primary infection in promoting memory differentiation and longevity. We noted that endogenous responders with higher functional avidity were more likely to transition from effector cells to memory cells (Figures 6A and 6B). Even a monoclonal population of SMARTA cells displayed a skewing toward higher functional avidity in the transition to memory after LCMV infection (Figure 6C), agreeing with studies indicating that responding T cells can distribute over a range of functional avidities regardless of TCR affinity (Kroger and Alexander-Miller, 2007; Slifka and Whitton, 2001). Furthermore, endogenous memory cells generated by either LCMV or Lm-gp61 infection displayed a continuous skewing over time toward higher functional avidity (Figures 6D and 6E). Although the overall population of memory cells decreases in number over time, those memory cells with higher functional avidity survive preferentially. To illustrate this, if only the numbers of responders with high functional avidity (i.e., those that respond to peptide concentrations $\leq 1 \times 10^{-8}$ M) are plotted over time, they display virtually no decay during the memory maintenance phase (Figure S7). These findings suggest that the strength of the stimulatory signal delivered to $CD4^+$ T cells during the primary response can dictate not only recruitment into the response, but also memory differentiation and the subsequent longevity of memory cell populations.

DISCUSSION

Our data, plus those of others, show that SMARTA cells are an ideal model to follow the in vivo response to LCMV infection through the expansion, contraction, and memory phases (Whitmire et al., 2006). However, after infection with recombinant *Listeria* expressing the LCMV epitope, we found that even though the SMARTA expansion phase was intact, the effector population rapidly contracted to zero and left no memory cells. In mice in which the frequency of SMARTA cells approached the endogenous precursor frequency for the gp_{61-80} epitope,

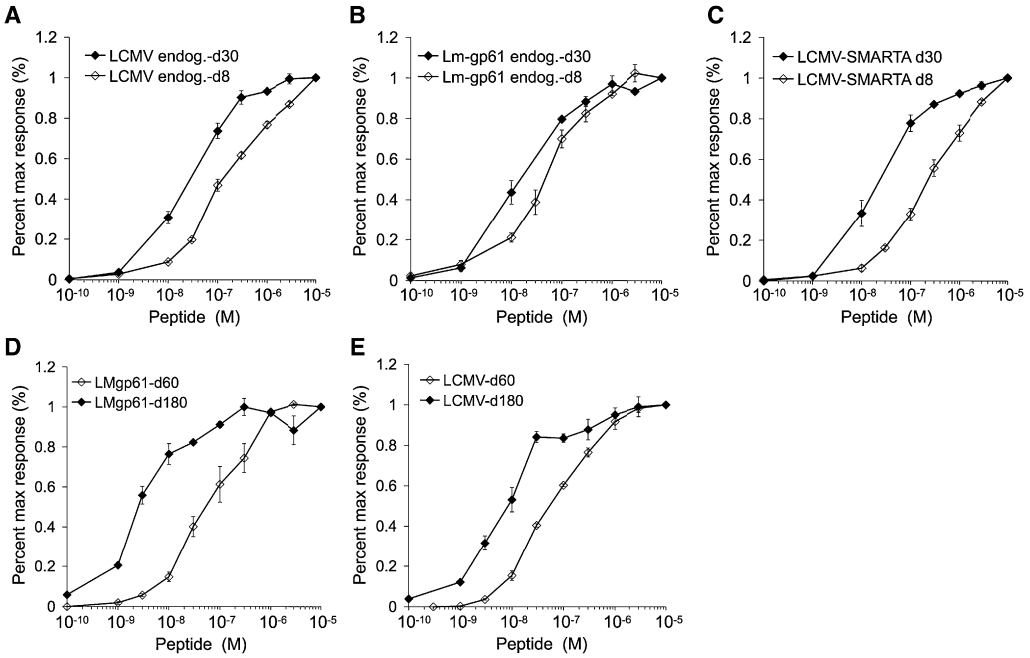

Figure 6. CD4$^+$ Memory T Cells Skew to Higher Functional Avidity over Time

(A) B6 mice were infected with LCMV. At 8 or 30 days p.i., splenocytes were restimulated over a range of $GP_{61–80}$ peptide concentrations ex vivo and stained for expression of IFNγ and TNFα. The graph displays the percent maximal endogenous CD4$^+$ T cell response induced by ex vivo peptide restimulation, as measured by the frequency of cytokine-producing responders at each peptide concentration divided by the frequency of cytokine-producing responders at the highest peptide concentration (1×10^{-5} M).

(B) Similar experiments were performed after Lm-gp61 infection.

(C) Similar experiments were performed as in (A), except that 1×10^4 CD44^{lo} SMARTA cells were transferred 1 day prior to LCMV infection and the functional avidity of Thy1.1$^+$ SMARTA cells was assessed.

(D and E) Experiments similar to those in (A) and (B) were performed, except that functional avidity was assessed at days 60 and 180 p.i.

All error bars represent the SEM (n = 3–4 per group).

SMARTA cells expanded 12,000- to 20,000-fold, representing at least 12–14 cell divisions, but by day 15 p.i. 100% of the cells had died. Meanwhile, in the same mice, there was an apparently normal expansion, contraction, and memory response by the endogenous CD4$^+$ T cell population. Even by day 5 p.i., before demonstrating defects in cytokine production, SMARTA cells had entered an irreversible pathway of programmed cell death that could not be reversed by LCMV challenge. These results indicate that sufficient signaling for clonal expansion and at least partial differentiation of effector function can occur without receiving the signals required for memory differentiation.

In vitro studies have led to a model of progressive differentiation in which T cell fitness and survival are dependent on the strength of the antigenic stimulus (Gett et al., 2003; Lanzavecchia and Sallusto, 2002). More recent in vivo studies of the CD8$^+$ T cell response have instead suggested a model of programmed differentiation, in which a short encounter with antigen promotes the antigen-independent expansion and differentiation of responding T cells (Prlic et al., 2007; Kaech and Wherry, 2007). CD4$^+$ T cells, however, appear to require a more extended period of antigen stimulation for the induction of a robust response (Obst et al., 2005; Williams and Bevan, 2004). This is supported by the observation that CD4$^+$ T cell responders undergo functional-avidity maturation throughout the primary response (Whitmire et al., 2006). Also, the progressive skewing toward a high-avidity repertoire throughout both primary and secondary CD4$^+$ T cell responses suggests an extended period of antigen-driven repertoire selection (Savage et al., 1999). Our results support a model in which increasing degrees of antigenic stimulation promote hierarchical stages of differentiation. Increasing stimulation would first promote clonal expansion and subsequently effector differentiation, differentiation of short-lived memory cells, and finally differentiation of long-lived memory cells. The inability of SMARTA cells to differentiate into memory after Lm-gp61 infection, despite their massive clonal expansion and initial development of effector function, correlates with a lower range of functional and TCR avidity of SMARTA cells compared to the endogenous CD4$^+$ T cell responders to the same epitope. Because the avidity of responding T cell populations has been shown to inversely correlate with antigen dose (Rees et al., 1999), we suggest that the inability of SMARTA cells to receive proper signals for memory differentiation after Lm-gp61 challenge may be due to limited antigen availability. The observation that memory SMARTA rechallenged with Lm-gp61 differentiate normally and form secondary memory fits with the notion that memory cells have a lower activation threshold and can be more efficiently recruited by lower amounts of antigen.

Several explanations for decreased antigen availability may be proposed, including decreased antigen display on APCs, clonal competition, and competition with other immunodominant epitopes. Of these, we have ruled out clonal competition as a mechanism for regulating the degree of antigen stimulation in this

particular system, although it has been recently reported that in other scenarios clonal competition inhibited both $CD4^+$ T cell memory differentiation and maintenance (Blair and Lefrancois, 2007; Hataye et al., 2006). The inability of SMARTA cells to differentiate into memory after Lm-gp61 infection does not necessarily represent an abnormal differentiation event. Rather, during Lm-gp61 infection, SMARTA cells represent clones that normally expand after activation but do not receive sufficient TCR signals for memory differentiation. SMARTA cells may thus provide a snapshot of one differentiation stage during Lm-gp61 infection and highlight the heterogeneous nature of the effector $CD4^+$ T cell population.

We definitively show that the disappearance of SMARTA cells after Lm-gp61 infection is not due to a rejection artifact peculiar to Lm-gp61 infection but represents a genuine differentiation defect. In all, these results provide a comprehensive picture of $CD4^+$ T cell differentiation during an immune response in which the signaling threshold for clonal expansion is met prior to those for effector differentiation and development of short-lived and long-lived memory populations. Antigen-driven signals do not represent the whole story, however, for even among the $CD4^+$ T cell responders of the highest functional avidity substantial contraction is observed, indicating that other signals are required for the differentiation of $CD4^+$ memory T cells. Also, it is unclear to what extent these findings are influenced by the distinct inflammatory environments of each infection model. Differences in the inflammatory milieu may have substantial effects on T cell differentiation. Recent studies have found that signaling by inflammatory mediators such as IL-12 or type I IFNs can preferentially promote end-stage effector differentiation of $CD8^+$ T cells (Pearce and Shen, 2007; Joshi et al., 2007). We observe normal differentiation of endogenous responders and of memory SMARTA rechallenged with Lm-gp61, arguing against the possibility that the inflammatory environment is the determining factor for memory differentiation in our system. Furthermore, we observe defective effector differentiation at the peak of the response, indicating that the defect in SMARTA cells goes beyond a switch from a memory differentiation pathway to an effector differentiation pathway. Future studies are needed to assess the impact of modulating antigen presentation while keeping the bystander inflammatory environment constant.

Notably, Bim expression was increased in SMARTA effector cells after Lm-gp61 infection. Bim is required during the contraction phase of the immune response (Pellegrini et al., 2003; Wojciechowski et al., 2006) and influences other aspects of naive and memory T cell homeostasis (Wojciechowski et al., 2007; Hughes et al., 2008; Hutcheson et al., 2008; Weant et al., 2008). One intriguing possibility is that the extent of antigen stimulation may influence Bim expression in $CD4^+$ T cells. However, Bim is not differentially expressed in SMARTA cells until day 7 p.i. (data not shown). Although Bim upregulation may explain the disappearance of SMARTA cells after Lm-gp61 infection, it does not explain the loss of cytokine-producing capability nor the inability of SMARTA cells to respond to further antigenic signals at earlier time points. It remains possible that Bim is a crucial mediator of T cell death caused by insufficient TCR-mediated differentiation signals, but it is also possible that Bim is only one byproduct of a differentiation program gone awry.

It has recently been shown that in some mouse models $CD4^+$ memory T cell populations do not share the stability of $CD8^+$ memory T cell populations, declining slowly over time (Homann et al., 2001). In our studies of $CD4^+$ T cell memory, we have also observed a steady, if slow, decline in $CD4^+$ T cell memory populations, both by endogenous and SMARTA memory cells. However, the rate of decline slowed over time, and we were unable to detect a decline in endogenous memory cells beyond 6 months p.i. Also, surviving memory cell populations consistently skewed to an ever-higher functional avidity. This may represent the outgrowth of clones with high functional avidity or the functional maturation of the memory population as a whole. Secondary challenge of mice has been shown to select for responding clones with high avidity (Rees et al., 1999), suggesting that the skewing we observe is probably attributable to the preferential survival of memory cells with high functional avidity. These data suggest that not only does TCR signal strength during the primary response impact the generation of $CD4^+$ T cell memory, but it also influences the longevity $CD4^+$ T cell memory populations. We propose that long-lived $CD4^+$ memory T cells represent those responders that received the strongest stimulus during the primary response. This also differs from implications for $CD8^+$ memory T cells, for which it is suggested that excessive stimulation, from either antigen or inflammatory mediators, drives the differentiation of end-stage effector CTL that have lost the capacity for memory differentiation (Joshi et al., 2007). In these settings, it is likely that increasing degrees of stimulation decrease $CD8^+$ memory T cell differentiation potential, the opposite of the scenario we envisage for $CD4^+$ T cells.

In summary, our data indicate that the signals that induce massive clonal expansion of $CD4^+$ T cells after primary activation are distinct from those that induce memory differentiation. We propose that increasing the strength of antigenic signals promotes hierarchical differentiation of $CD4^+$ T cell responders, with the most profound activation signals leading to the formation of stable $CD4^+$ memory T cell populations. Further studies should elucidate the precise role of antigen-driven stimulation in memory development, as well as the functional consequences of an emerging, narrower repertoire of high-avidity $CD4^+$ memory T cells.

EXPERIMENTAL PROCEDURES

Mice and Infections

Six- to eight-week-old C57BL/6 mice were purchased from Jackson Laboratories (Bar Harbor, ME). SMARTA TCR transgenic mice (Oxenius et al., 1998) were maintained in SPF facilities at the University of Washington and the University of Utah. All animal experiments were conducted with the approval of the corresponding animal use committees (IACUC) at each institution. LCMV Armstrong 53b was grown in BHK cells and titered in Vero cells as described (Ahmed et al., 1984). Mice were infected intraperitoneally (i.p.) with 2×10^5 plaque-forming units (PFU). Lm-gp61 expressing the gp_{61-80} epitope of LCMV (a gift from M. Kaja-Krishna, University of Washington, Seattle, WA) (Way et al., 2007) was constructed via described methods (Shen et al., 1995) and propagated in BHI broth and on agar plates. Prior to infection, the bacteria were grown to log phase and concentration determined by measuring the O.D. at 600 nm (O.D. of $1 = 1 \times 10^9$ CFU/ml). Mice were injected intravenously (i.v.) with 2×10^5 colony-forming units (CFU). All mouse experiments were performed in accordance with protocols approved by the IACUC at the University of Washington and the University of Utah.

Adoptive Transfers

Splenocyte cell suspensions were generated from SMARTA mice. Untouched $CD4^+$ T cells were isolated by incubation with a biotinylated antibody cocktail followed by antibiotin magnetic beads and depletion on a magnetic column,

per manufacturer's recommendations (Miltenyi). In addition, we added biotinylated CD44 antibody (eBiosciences, San Diego, CA) to deplete CD44^{hi} "memory phenotype" SMARTA. TCR transgenic T cell purity was assessed by staining with CD44, Vα2, and Vβ8.3 antibodies, followed by flow-cytometric analysis. SMARTA cells were resuspended in PBS and injected i.v. into recipient mice 1 day prior to infection. In some experiments, SMARTA cells were incubated with 5 mM 5-(and-6)-carboxyfluorescein diacetate, succinimidyl ester (CFSE) (Invitrogen) for 10 min in warm RPMI.

Microarray and RT-PCR

RNA was isolated with Trizol (Invitrogen) from FACS-sorted SMARTA cells (day 8 p.i.). Message was amplified and converted to biotinylated, fragmented cRNA with a commercially available kit per manufacturer's instructions (Ambion, Austin, TX). Two biological duplicates from each group were hybridized to Affymetrix Mouse 430 2.0 arrays. Results were normalized (GC-RMA, Bioconducter) and analyzed for differences in $\log_2$ expression values. Target genes were identified for further study on the basis of > 2.5-fold increased expression in two separate experiments, with a minimum mean of ≥ 3-fold increased expression. For RT-PCR, first-strand cDNA synthesis and SYBR-green based analysis of real-time PCR amplification was performed with a commercially available kit (Invitrogen) and a Lightcycler 480 (Roche). The following exon-spanning primer pairs were used (5′→3′): Bim: forward-CGGATCGGAGACGAGTTCA, reverse-TTCAGCCTCGCGGTAATCA-; Nor-1: forward-GATCACAGAGCGACATGGGTTA, reverse-GAGCCTGTCCCTTCC TCTGG; Bcl-2: forward-GTGGTGGAGGAACTCTTCAGGGATG, reverse-GG TCTTCAGAGACAGCCAGGAGAAATC; TCF-1: forward-AGTCCCACAGTGT CCTCCAG, reverse-CACGGTTACTGGGAAGAGGA; and β-catenin: forward-CCCTGAGACGCTAGATGAGG; reverse-CATGATGGCATGTCTGGAAG. Expression was normalized to GAPDH or HPRT and displayed as a relative n-fold increase.

Ex Vivo Restimulation and Intracellular Cytokine Staining

Splenocyte cell suspensions in RPMI supplemented with 10% fetal bovine serum were plated in round-bottom 96-well plates (2–3 × 10^6 cells/well) and restimulated for 4 hr with 1 μM (or titrated dilutions as indicated in the pertinent figures) $GP_{61–80}$ peptide from LCMV (GLKGPDIYKGVYQFKSVEFD) in the presence of Brefeldin A (GolgiPlug, 1 μl/ml), per manufacturer's instructions (BD Biosciences, San Diego, CA). After restimulation, cells were stained with fluorescently labeled cell-surface antibodies to CD4 and Thy1.1, permeabilized, and stained with fluorescently labeled antibodies to IFNγ, TNFα, and IL-2, with a kit per manufacturer's instructions (BD Biosciences, San Diego, CA). Samples were then analyzed by flow cytometry.

Tetramer Staining and Analysis

The $gp_{66–77}$:I-A^b tetramer was provided by the NIH Tetramer Core Facility (Emory Vaccine Center, Atlanta, GA). Staining was performed at 37°C for 3 hr in RPMI containing 2% FCS, followed by washing and cell-surface staining for CD4, CD44 and Thy1.1. Tetramer fluorescence was normalized to samples stained with control tetramer, hCLIP:I-A^b. Scatchard plots and apparent K_D were calculated as described (Savage et al., 1999). Fluorescence units (bound) were plotted on the x axis, and fluorescence units divided by tetramer concentration (bound/free) were plotted on the y axis. K_D was determined as the inverse of the slope.

Antibodies and Flow Cytometry

Cell-surface stains were done in PBS containing 1% FBS. Intracellular stains for cytokines and Bcl-2 were done with a kit per manufacturer's instructions (BD Biosciences). Antibodies conjugated to fluorescent labels were purchased from eBiosciences (San Diego, CA) and include CD4, Thy1.1, IFNγ, IL-2, TNFα, CD62L, and CD44. Antibodies purchased from BD Biosciences (Mountain View, CA) include Bcl-2-PE, Vα2-PE, Vβ8.3-FITC, and the Vβ panel-staining kit. Flow cytometry was performed with either a FACSCalibur or a FACSCanto, and high-speed cell sorting was performed with either a FACSVantage or a FACSAria (BD Biosciences).

ACCESSION NUMBERS

Microarray data have been submitted to the online depository GEO (accession# GSE10094) and conform to all MIAME guidelines.

SUPPLEMENTAL DATA

Seven figures are available at http://www.immunity.com/cgi/content/full/28/4/533/DC1/.

ACKNOWLEDGMENTS

The authors wish to acknowledge B. Dere, P. Xiao, and J. Strickland for technical assistance. We also gratefully acknowledge the National Institutes of Health (NIH) Tetramer Core Facility (Atlanta, GA) for providing MHC Class II tetramers. This research was supported by the NIH (M.A.W) and the Howard Hughes Medical Institute (M.J.B.).

Received: October 16, 2007
Revised: January 17, 2008
Accepted: February 6, 2008
Published online: March 20, 2008

REFERENCES

Ahmed, R., Salmi, A., Butler, L.D., Chiller, J.M., and Oldstone, M.B. (1984). Selection of genetic variants of lymphocytic choriomeningitis virus in spleens of persistently infected mice. Role in suppression of cytotoxic T lymphocyte response and viral persistence. J. Exp. Med. *160*, 521–540.

Bachmann, M.F., Wolint, P., Walton, S., Schwarz, K., and Oxenius, A. (2007). Differential role of IL-2R signaling for CD8+ T cell responses in acute and chronic viral infections. Eur. J. Immunol. *37*, 1502–1512.

Bitomsky, N., Bohm, M., and Klempnauer, K.H. (2004). Transformation suppressor protein Pdcd4 interferes with JNK-mediated phosphorylation of c-Jun and recruitment of the coactivator p300 by c-Jun. Oncogene *23*, 7484–7493.

Blair, D.A., and Lefrancois, L. (2007). Increased competition for antigen during priming negatively impacts the generation of memory CD4 T cells. Proc. Natl. Acad. Sci. USA *104*, 15045–15050.

Breitfeld, D., Ohl, L., Kremmer, E., Ellwart, J., Sallusto, F., Lipp, M., and Forster, R. (2000). Follicular B helper T cells express CXC chemokine receptor 5, localize to B cell follicles, and support immunoglobulin production. J. Exp. Med. *192*, 1545–1552.

Chen, J., Yusuf, I., Andersen, H.-M., and Fruman, D.A. (2006). FOXO transcription factors cooperate with {delta}EF1 to activate growth suppressive genes in B lymphocytes. J. Immunol. *176*, 2711–2721.

Cheng, L.E., Chan, F.K., Cado, D., and Winoto, A. (1997). Functional redundancy of the Nur77 and Nor-1 orphan steroid receptors in T-cell apoptosis. EMBO J. *16*, 1865–1875.

Christian, S.L., Lee, R.L., McLeod, S.J., Burgess, A.E., Li, A.H.Y., Dang-Lawson, M., Lin, K.B.L., and Gold, M.R. (2003). Activation of the Rap GTPases in B lymphocytes modulates B cell antigen receptor-induced activation of Akt but has no effect on MAPK activation. J. Biol. Chem. *278*, 41756–41767.

Foulds, K.E., and Shen, H. (2006). Clonal competition inhibits the proliferation and differentiation of adoptively transferred TCR transgenic CD4 T cells in response to infection. J. Immunol. *176*, 3037–3043.

Gett, A.V., Sallusto, F., Lanzavecchia, A., and Geginat, J. (2003). T cell fitness determined by signal strength. Nat. Immunol. *4*, 355–360.

Green, D.R., Droin, N., and Pinkoski, M. (2003). Activation-induced cell death in T cells. Immunol. Rev. *193*, 70–81.

Hammarlund, E., Lewis, M.W., Hansen, S.G., Strelow, L.I., Nelson, J.A., Sexton, G.J., Hanifin, J.M., and Slifka, M.K. (2003). Duration of antiviral immunity after smallpox vaccination. Nat. Med. *9*, 1131–1137.

Hand, T.W., Morre, M., and Kaech, S.M. (2007). Expression of IL-7 receptor {alpha} is necessary but not sufficient for the formation of memory CD8 T cells during viral infection. Proc. Natl. Acad. Sci. USA *104*, 11730–11735.

Hataye, J., Moon, J.J., Khoruts, A., Reilly, C., and Jenkins, M.K. (2006). Naive and memory CD4+ T cell survival controlled by clonal abundance. Science *312*, 114–116.

Hendriks, J., Xiao, Y., and Borst, J. (2003). CD27 promotes survival of activated T cells and complements CD28 in generation and establishment of the effector T cell pool. J. Exp. Med. *198*, 1369–1380.

Homann, D., Teyton, L., and Oldstone, M.B.A. (2001). Differential regulation of antiviral T-cell immunity results in stable CD8+ but declining CD4+ T-cell memory. Nat. Med. *7*, 913–919.

Hughes, P.D., Belz, G.T., Fortner, K.A., Budd, R.C., Strasser, A., and Bouillet, P. (2008). Apoptosis regulators Fas and Bim cooperate in shutdown of chronic immune responses and prevention of autoimmunity. Immunity *28*, 197–205.

Hutcheson, J., Scatizzi, J.C., Siddiqui, A.M., Haines, G.K., Wu, T., Li, Q., Davis, L.S., Mohan, C., and Perlman, H. (2008). Combined deficiency of proapoptotic regulators Bim and Fas results in the early onset of systemic autoimmunity. Immunity *28*, 206–217.

Janssen, E.M., Lemmens, E.E., Wolfe, T., Christen, U., von Herrath, M.G., and Schoenberger, S.P. (2003). CD4+ T cells are required for secondary expansion and memory in CD8+ T lymphocytes. Nature *421*, 852–856.

Jia, S., and Meng, A. (2007). Tob genes in development and homeostasis. Dev. Dyn. *236*, 913–921.

Jiang, Y., Woronicz, J.D., Liu, W., and Goeddel, D.V. (1999). Prevention of constitutive TNF receptor 1 signaling by silencer of death domains. Science *283*, 543–546.

Joshi, N.S., Cui, W., Chandele, A., Lee, H.K., Urso, D.R., Hagman, J., Gapin, L., and Kaech, S.M. (2007). Inflammation directs memory precursor and short-lived effector CD8+ T cell fates via the graded expression of T-bet transcription factor. Immunity *27*, 281–295.

Kabashima, K., Saji, T., Murata, T., Nagamachi, M., Matsuoka, T., Segi, E., Tsuboi, K., Sugimoto, Y., Kobayashi, T., Miyachi, Y., et al. (2002). The prostaglandin receptor EP4 suppresses colitis, mucosal damage and CD4 cell activation in the gut. J. Clin. Invest. *109*, 883–893.

Kaech, S.M., and Ahmed, R. (2001). Memory CD8+ T cell differentiation: Initial antigen encounter triggers a developmental program in naive cells. Nat. Immunol. *2*, 415–422.

Kaech, S.M., Tan, J.T., Wherry, E.J., Konieczny, B.T., Surh, C.D., and Ahmed, R. (2003). Selective expression of the interleukin 7 receptor identifies effector CD8 T cells that give rise to long-lived memory cells. Nat. Immunol. *4*, 1191–1198.

Kaech, S.M., and Wherry, E.J. (2007). Heterogeneity and cell-fate decisions in effector and memory CD8+ T cell differentiation during viral infection. Immunity *27*, 393–405.

Kester, H.A., Blanchetot, C., den Hertog, J., van der Saag, P.T., and van der Burg, B. (1999). Transforming growth factor-beta -stimulated clone-22 is a member of a family of leucine zipper proteins that can homo- and heterodimerize and has transcriptional repressor activity. J. Biol. Chem. *274*, 27439–27447.

Klonowski, K.D., Williams, K.J., Marzo, A.L., and Lefrancois, L. (2006). Cutting edge: IL-7-independent regulation of IL-7 receptor {alpha} expression and memory CD8 T cell development. J. Immunol. *177*, 4247–4251.

Kroger, C.J., and Alexander-Miller, M.A. (2007). Cutting edge: CD8+ T cell clones possess the potential to differentiate into both high- and low-avidity effector cells. J. Immunol. *179*, 748–751.

Lanzavecchia, A., and Sallusto, F. (2002). Progressive differentiation and selection of the fittest in the immune response. Nat. Rev. Immunol. *2*, 982–987.

Liang, H., Samanta, S., and Nagarajan, L. (2005). SSBP2, a candidate tumor suppressor gene, induces growth arrest and differentiation of myeloid leukemia cells. Oncogene *24*, 2625–2634.

Lin, L., Hron, J.D., and Peng, S.L. (2004). Regulation of NF-kappaB, Th Activation, and autoinflammation by the forkhead transcription factor Foxo3a. Immunity *21*, 203–213.

Mamura, M., Nakao, A., Goto, D., Kato, M., Saito, Y., and Iwamoto, I. (2000). Ligation of the T cell receptor complex results in phosphorylation of Smad2 in T lymphocytes. Biochem. Biophys. Res. Commun. *268*, 124–127.

Marrack, P., and Kappler, J. (2004). Control of T cell viability. Annu. Rev. Immunol. *22*, 765–787.

Mercado, R., Vijh, S., Allen, S.E., Kerksiek, K., Pilip, I.M., and Pamer, E.G. (2000). Early programming of T cell populations responding to bacterial infection. J. Immunol. *165*, 6833–6839.

Metcalfe, S.M., Muthukumarana, P.A.D.S., Thompson, H.L., Haendel, M.A., and Lyons, G.E. (2005). Leukaemia inhibitory factor (LIF) is functionally linked to axotrophin and both LIF and axotrophin are linked to regulatory immune tolerance. FEBS Lett. *579*, 609–614.

Muto, A., Tashiro, S., Tsuchiya, H., Kume, A., Kanno, M., Ito, E., Yamamoto, M., and Igarashi, K. (2002). Activation of Maf/AP-1 repressor Bach2 by oxidative stress promotes apoptosis and its interaction with promyelocytic leukemia nuclear bodies. J. Biol. Chem. *277*, 20724–20733.

Myers, M.D., Dragone, L.L., and Weiss, A. (2005). Src-like adaptor protein down-regulates T cell receptor (TCR)-CD3 expression by targeting TCR{zeta} for degradation. J. Cell Biol. *170*, 285–294.

Obst, R., van Santen, H.-M., Mathis, D., and Benoist, C. (2005). Antigen persistence is required throughout the expansion phase of a CD4+ T cell response. J. Exp. Med. *201*, 1555–1565.

Onami, T.M., Harrington, L.E., Williams, M.A., Galvan, M., Larsen, C.P., Pearson, T.C., Manjunath, N., Baum, L.G., Pearce, B.D., and Ahmed, R. (2002). Dynamic regulation of T cell immunity by CD43. J. Immunol. *168*, 6022–6031.

Oxenius, A., Bachmann, M.F., Zinkernagel, R.M., and Hengartner, H. (1998). Virus-specific MHC-class II-restricted TCR-transgenic mice: Effects on humoral and cellular immune responses after viral infection. Eur. J. Immunol. *28*, 390–400.

Parry, R.V., Chemnitz, J.M., Frauwirth, K.A., Lanfranco, A.R., Braunstein, I., Kobayashi, S.V., Linsley, P.S., Thompson, C.B., and Riley, J.L. (2005). CTLA-4 and PD-1 receptors inhibit T-cell activation by distinct mechanisms. Mol. Cell. Biol. *25*, 9543–9553.

Pearce, E.L., and Shen, H. (2007). Generation of CD8 T cell memory is regulated by IL-12. J. Immunol. *179*, 2074–2081.

Pellegrini, M., Belz, G., Bouillet, P., and Strasser, A. (2003). Shutdown of an acute T cell immune response to viral infection is mediated by the proapoptotic Bcl-2 homology 3-only protein Bim. Proc. Natl. Acad. Sci. USA *100*, 14175–14180.

Prlic, M., Hernandez-Hoyos, G., and Bevan, M.J. (2006). Duration of the initial TCR stimulus controls the magnitude but not functionality of the CD8+ T cell response. J. Exp. Med. *203*, 2135–2143.

Prlic, M., Williams, M.A., and Bevan, M.J. (2007). Requirements for CD8 T-cell priming, memory generation and maintenance. Curr. Opin. Immunol. *19*, 315–319.

Qiang, Y.W., and Rudikoff, S. (2004). Wnt signaling in B and T lymphocytes. Front. Biosci. *9*, 1000–1010.

Rees, W., Bender, J., Teague, T.K., Kedl, R.M., Crawford, F., Marrack, P., and Kappler, J. (1999). An inverse relationship between T cell receptor affinity and antigen dose during CD4+ T cell responses in vivo and in vitro. Proc. Natl. Acad. Sci. USA *96*, 9781–9786.

Savage, P.A., Boniface, J.J., and Davis, M.M. (1999). A kinetic basis for T cell receptor repertoire selection during an immune response. Immunity *10*, 485–492.

Schaerli, P., Willimann, K., Lang, A.B., Lipp, M., Loetscher, P., and Moser, B. (2000). CXC chemokine receptor 5 expression defines follicular homing T cells with B cell helper function. J. Exp. Med. *192*, 1553–1562.

Scott, K.L., and Plon, S.E. (2005). CHES1/FOXN3 interacts with Ski-interacting protein and acts as a transcriptional repressor. Gene *359*, 119–126.

Shedlock, D.J., and Shen, H. (2003). Requirement for CD4 T cell help in generating functional CD8 T cell memory. Science *300*, 337–339.

Shen, H., Slifka, M.K., Matloubian, M., Jensen, E.R., Ahmed, R., and Miller, J.F. (1995). Recombinant *Listeria monocytogenes* as a live vaccine vehicle for the induction of protective anti-viral cell-mediated immunity. Proc. Natl. Acad. Sci. USA *92*, 3987–3991.

Slifka, M.K., and Whitton, J.L. (2001). Functional avidity maturation of CD8+ T cells without selection of higher affinity TCR. Nat. Immunol. *2*, 711–717.

Stahl, M., Dijkers, P.F., Kops, G.J.P.L., Lens, S.M.A., Coffer, P.J., Burgering, B.M.T., and Medema, R.H. (2002). The Forkhead transcription factor FoxO

regulates transcription of p27Kip1 and Bim in response to IL-2. J. Immunol. *168*, 5024–5031.

Sun, J.C., and Bevan, M.J. (2003). Defective CD8 T cell memory following acute infection without CD4 T cell help. Science *300*, 339–342.

Sun, J.C., Lehar, S.M., and Bevan, M.J. (2006). Augmented IL-7 signaling during viral infection drives greater expansion of effector T cells but does not enhance memory. J. Immunol. *177*, 4458–4463.

van Stipdonk, M.J.B., Hardenberg, G., Bijker, M.S., Lemmens, E.E., Droin, N.M., Green, D.R., and Schoenberger, S.P. (2003). Dynamic programming of CD8+ T lymphocyte responses. Nat. Immunol. *4*, 361–365.

Vietor, I., and Huber, L.A. (2007). Role of TIS7 family of transcriptional regulators in differentiation and regeneration. Differentiation *75*, 891–897.

Waldmann, T.A. (2006). The biology of interleukin-2 and interleukin-15: Implications for cancer therapy and vaccine design. Nat. Rev. Immunol. *6*, 595–601.

Way, S.S., Havenar-Daughton, C., Kolumam, G.A., Orgun, N.N., and Murali-Krishna, K. (2007). IL-12 and type-I IFN synergize for IFN-gamma production by CD4 T cells, whereas neither are required for IFN-gamma production by CD8 T cells after *Listeria monocytogenes* infection. J. Immunol. *178*, 4498–4505.

Weant, A.E., Michalek, R.D., Khan, I.U., Holbrook, B.C., Willingham, M.C., and Grayson, J.M. (2008). Immunity *28*, 218–230.

Whitmire, J.K., Benning, N., and Whitton, J.L. (2006). Precursor frequency, nonlinear proliferation, and functional maturation of virus-specific CD4+ T cells. J. Immunol. *176*, 3028–3036.

Williams, M.A., and Bevan, M.J. (2004). Shortening the infectious period does not alter expansion of CD8 T cells but diminishes their capacity to differentiate into memory cells. J. Immunol. *173*, 6694–6702.

Williams, M.A., and Bevan, M.J. (2007). Effector and memory CTL differentiation. Annu. Rev. Immunol. *25*, 171–192.

Williams, M.A., Tyznik, A.J., and Bevan, M.J. (2006). Interleukin-2 signals during priming are required for secondary expansion of CD8+ memory T cells. Nature *441*, 890–893.

Wojciechowski, S., Jordan, M.B., Zhu, Y., White, J., Zajac, A.J., and Hildeman, D.A. (2006). Bim mediates apoptosis of CD127(lo) effector T cells and limits T cell memory. Eur. J. Immunol. *36*, 1694–1706.

Wojciechowski, S., Tripathi, P., Bourdeau, T., Acero, L., Grimes, H.L., Katz, J.D., Finkelman, F.D., and Hildeman, D.A. (2007). Bim/Bcl-2 balance is critical for maintaining naive and memory T cell homeostasis. J. Exp. Med. *204*, 1665–1675.

Yamagishi, N., Ishihara, K., Saito, Y., and Hatayama, T. (2006). Hsp105 family proteins suppress staurosporine-induced apoptosis by inhibiting the translocation of Bax to mitochondria in HeLa cells. Exp. Cell Res. *312*, 3215–3223.

Zhang, J., Xu, L.-G., Han, K.-J., and Shu, H.-B. (2004). Identification of a ZU5 and death domain-containing inhibitor of NF-{kappa}B. J. Biol. Chem. *279*, 17819–17825.